DALTON

Synthesis and characterisation of a *semipseudocloso* carbaruthenaborane. Molecular structure of [1-(PhCC)-2-Ph-3-(cym)-3,1,2-*semipseudocloso*-$RuC_2B_9H_9$] (cym = *p*-cymene)*

Rhodri Ll. Thomas and Alan J. Welch

Department of Chemistry, Heriot-Watt University, Edinburgh EH14 4AS, UK

The *closo* carbaborane 1-(PhCC)-2-Ph-1,2-$C_2B_{10}H_{10}$ was readily decapitated to afford either [7-(PhCC)-8-Ph-7,8-$C_2B_9H_{10}$]$^-$ or [7-(PhCC)-8-Ph-7,8-$C_2B_9H_9$]$^{2-}$. Reaction of the thallium(I) salt of the latter with [{$RuCl_2$(cym)}$_2$] (cym = *p*-cymene) yielded the unique *semipseudocloso* carbaruthenaborane [1-(PhCC)-2-Ph-3-(cym)-3,1,2-$RuC_2B_9H_9$] characterised by multinuclear NMR spectroscopy (weighted average ^{11}B chemical shift +2.41 ppm) and by single-crystal X-ray diffraction [C(1)–C(2) 2.184(7), Ru(3) · · · B(6) 3.166(6) Å]. The *semipseudocloso* shape thus appears to lie between *closo* and *pseudocloso*, although somewhat closer to the latter. Confirmation of the structure strongly supports the idea of a continuum of cluster structures from *closo* to *pseudocloso*, the position of a molecule on which may be controlled by steric effects.

We have recently demonstrated that intramolecular steric crowding in heteroboranes can lead to unusual molecular structures. Thus, whilst the conformations of the phenyl rings, θ_{Ph} (the modulus of the average C_{cage}–C_{cage}–C_{Ph}–C_{Ph} torsion angle) in 1,2-Ph_2-1,2-*closo*-$C_2B_{10}H_{10}$ [2] and [7,8-Ph_2-7,8-*nido*-$C_2B_9H_{10}$]$^{-}$ [3] are typically low, allowing the expected *closo* geometries to be observed, θ_{Ph} increases substantially when [7,8-Ph_2-7,8-*nido*-$C_2B_9H_9$]$^{2-}$ is bound to conical transition-metal-containing fragments such as {(η^5-L)M} (L = C_5Me_5, M = Rh [4] or Ir;[5] L = C_9Me_7, M = Rh [6]), {(η^6-L)M} [L = C_6H_6, $MeC_6H_4Pr^i$-4 (*p*-cymene, cym) or C_6Me_6, M = Ru [5]] or {(κ^3-L)M} (L = 1,4,7-trithiacyclononane, M = Ru [7]). At high θ_{Ph} values the *ortho*-H · · · *ortho*-H crowding thereby generated prises apart the cage carbon atoms (typically to *ca.* 2.5 Å) and transforms the otherwise *closo* carbametallaborane **I** into a *pseudocloso* carbametallaborane **II**, in which the M(3)C(1)B(6)C(2) face is essentially square. Continuation of the deformation that leads from *closo* to *pseudocloso* ultimately recloses the M(3)C(1)B(6)C(2) face by making the M(3)–B(6) connectivity, generating a *hypercloso* species **III** from *closo* **I** by a single diamond–square–diamond step.

The *closo* to *pseudocloso* deformation appears to be accompanied by a movement to high frequency of the weighted average ^{11}B NMR chemical shift, ⟨δ(^{11}B)⟩, of the order of *ca.* 15 ppm, and, from individual boron resonance assignments *via* IGLO calculations [5] (IGLO = individual gauge for localised orbitals) and ^{11}B–^{11}B correlation spectroscopy (COSY) experiments [6] we were able to show that *all* boron resonances suffer a high-frequency shift, albeit to varying degrees. At the same time, determination of the molecular structure of the less crowded analogous species [1-Ph-2-Me-3-(cym)-3,1,2-$RuC_2B_9H_9$] and analysis of its ^{11}B NMR shifts both reveal the *beginnings* of a deformation from *closo* to *pseudocloso*, possibly suggesting that a structural continuum might exist between these forms.[8]

In the present contribution we confirm the existence of such a continuum by the synthesis and spectroscopic and crystallographic characterisation of [1-(PhCC)-2-Ph-3-(cym)-3,1,2-$RuC_2B_9H_9$]. This species displays a novel *semipseudocloso* polyhedral structure **IV**, essentially intermediate between *closo* and *pseudocloso*.

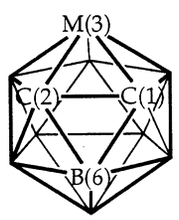

I *closo*

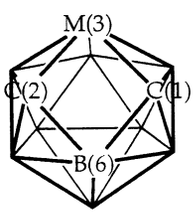

II *pseudocloso*

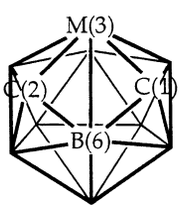

III *hypercloso*

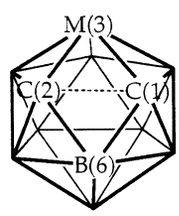

IV *semipseudocloso*

Experimental

Synthesis and spectroscopy

All reactions were carried out under an atmosphere of dry, oxygen-free nitrogen using standard Schlenk-line techniques, with some subsequent manipulations in the open laboratory. All solvents were dried and distilled under N_2 immediately prior to use. The NMR spectra were recorded at 298 K on Bruker AC 200 (^{1}H) and DPX 400 (^{11}B) spectrometers, chemical shifts being reported relative to external $SiMe_4$ (^{1}H) or BF_3·OEt_2 (^{11}B). Infrared spectra were recorded from CH_2Cl_2 solutions, referenced against the same solvent or, where indicated, as a KBr disc, on a Nicolet Impact 400 spectrophotometer. Microanalyses were performed by the Department of Applied Chemical and Physical Sciences, Napier University. The starting materials 1-(PhCC)-2-Ph-1,2-*closo*-$C_2B_{10}H_{10}$ [9] and [{$RuCl_2$(cym)}$_2$] [10] were prepared by literature methods or slight variants thereof.

Tl_2[7-(PhCC)-8-Ph-7,8-$C_2B_9H_9$]. The carbaborane 1-(PhCC)-

* Steric effects in heteroboranes. Part 15.[1]

2-Ph-1,2-$C_2B_{10}H_{10}$ (0.40 g, 1.25 mmol) was dissolved in ethanol (50 cm^3) and KOH (0.45 g, 8 mmol) was added. The solution was stirred for 30 min and then heated to reflux for 18 h. Solvent was removed under reduced pressure from the resultant pale yellow solution, to yield an oily solid. Addition of water (20 cm^3) gave a pale yellow suspension that was filtered through Celite®. Addition of a solution of thallium(I) acetate (2.10 g, 8 mmol) in water (5 cm^3) caused an immediate precipitation of a pale yellow solid. This was filtered off, and then washed with ethanol (2 × 5 cm^3) and diethyl ether (2 × 5 cm^3) followed by drying *in vacuo* to afford the product as a yellow solid. Yield 0.21 g, 24% (Found: C, 25.9; H, 2.3. Calc. for $C_{16}H_{19}B_9Tl_2$: C, 26.8; H, 2.65%). IR (KBr): ν_{max} at 2525 cm^{-1} (B–H).

[NEt_3H][7-(PhCC)-8-Ph-7,8-$C_2B_9H_{10}$]. To a solution of the carbaborane 1-(PhCC)-2-Ph-1,2-$C_2B_{10}H_{10}$ (1.80 g, 8.1 mmol) in ethanol (30 cm^3) was added KOH (0.92 g, 16.3 mmol). The solution was stirred for 30 min and then heated to reflux for 72 h. After cooling, saturation with CO_2 for 30 min gave a white precipitate which was filtered off. The solvent was removed from the filtrate under reduced pressure to afford an oily solid. To this was added water (20 cm^3), followed by a solution of triethylamine hydrochloride (2.33 g, 17 mmol) in water (5 cm^3). The resultant fine suspension was extracted into CH_2Cl_2 (3 × 25 cm^3) and dried over potassium carbonate. Filtration followed by removal of CH_2Cl_2 under reduced pressure gave a waxy white solid, that was recrystallised from Pr^iOH to yield the product [NEt_3H][7-(PhCC)-8-Ph-7,8-$C_2B_9H_{10}$] as a white powder. Yield 2.55 g, 76% (Found: C, 64.45; H, 8.85; N, 3.2. Calc. for $C_{22}H_{36}B_9N$: C, 64.2; H, 8.75; N, 3.4%). NMR $(CD_3)_2SO$: ^1H, δ 7.60–7.50 (m, 2 H, C_6H_5), 7.40–7.20 (m, 6 H, C_6H_5), 7.00–6.90 (m, 2 H, C_6H_5), 3.20 (q, 6 H, $^3J_{HH}$ = 8, NCH_2Me), 1.35 (t, 9 H, $^3J_{HH}$ = 8 Hz, CH_3) and −2.3 (br s, 1 H, *endo*-BH); ^{11}B-{^1H}, δ −4.34 (2B), −8.09 (1B), −13.70 (2B), −16.00 (1B), −16.82 (1B), −29.53 (1B) and −32.03 (1B).

[1-(PhCC)-2-Ph-3-(cym)-3,1,2-$RuC_2B_9H_9$] 2. A solution of [{$RuCl_2$(cym)}$_2$] (0.10 g, 0.18 mmol) in CH_2Cl_2 (20 cm^3) was cooled to −196 °C. To the frozen mass was added Tl_2[7-(PhCC)-8-Ph-7,8-$C_2B_9H_9$] (0.20 g, 0.3 mmol) and the mixture warmed to room temperature with stirring over 3 h. The resultant suspension was filtered through Celite®, affording an orange-red solution. Solvent was partially removed under reduced pressure, leaving 2–3 cm^3 of solution. Preparative TLC on SiO_2 using an eluent mixture [light petroleum (b.p. 40–60 °C)–CH_2Cl_2 (3:2)] gave one major mobile band, R_f = 0.4. This was isolated and recrystallised from CH_2Cl_2–light petroleum at −30 °C to give orange, diffractometer-quality crystals of 1-(PhCC)-2-Ph-3-(cym)-3,1,2-$RuC_2B_9H_9$ **2**. Yield 40 mg, 24% (Found: C, 57.5; H, 5.95. Calc. for $C_{26}H_{33}B_9Ru$: C, 57.45; H, 6.05%). IR (CH_2Cl_2): ν_{max} at 2580 cm^{-1} (B–H). NMR ($CDCl_3$): ^1H, δ 7.60–7.10 (m, 10 H, C_6H_5), 5.85–5.25 (m, 4 H, $MeC_6H_4CHMe_2$), 2.85 (spt, 1 H, $^3J_{HH}$ 7, $MeC_6H_4CHMe_2$), 1.90 (s, 3 H, $MeC_6H_4CHMe_2$) and 1.20 (d, 6 H, $^3J_{HH}$ 7 Hz, $MeC_6H_4CHMe_2$); ^{11}B-{^1H}, δ 21.89 (1B), 11.21 (1B), 4.95 (2B), −1.41 (4B) and −15.71 (1B).

Crystallography

Data for compound **2** were collected on a Siemens P4 diffractometer, using graphite-monochromated Mo-Kα X-radiation (λ = 0.710 69 Å). The unit-cell parameters were determined by the least-squares refinement of 31 reflections using XSCANS,[11] followed by a fractional index search. Crystallographic data and details of data collection and structure refinement are given in Table 1. Decay was monitored by regular measurements of the intensities of three high-intensity reflections, but was found not to be significant. Data were corrected for absorption effects by the use of ψ scans.[12] The structure was solved without difficulty by means of a Patterson map (Ru) followed by iterative least-squares refinement/Fourier-difference syntheses (all other non-H atoms).[13] Hydrogen atoms were placed in calculated positions, riding on the atom to which they are bound. After isotropic convergence, non-hydrogen atoms were allowed anisotropic thermal motion; U_H was set to 1.2 times the equivalent isotropic thermal parameter of the attached heavy atom (1.5 times U_{eq} for methyl groups). Towards the end of the refinement process data were weighted according to $w^{-1} = [\sigma^2(F_o^2) + (g_1P)^2 + (g_2P)]$ where $P = [\max(F_o^2 \text{ or } 0) + 2F_c^2]/3$ and g_1, g_2 are variables. The structure was refined to convergence by full-matrix least-squares refinement (on F^2). Geometrical calculations and molecular drawings were performed using SHELXTL.[13] Scattering factors for C, H, B and Ru were those inlaid in the programs.

Atomic coordinates, thermal parameters, and bond lengths and angles have been deposited at the Cambridge Crystallographic Data Centre (CCDC). See Instructions for Authors, *J. Chem. Soc., Dalton Trans.*, 1997, Issue 1. Any request to the CCDC for this material should quote the full literature citation and the reference number 186/346.

Results and Discussion

The carbaborane 1-(PhCC)-2-Ph-1,2-*closo*-$C_2B_{10}H_{10}$ is decapitated by KOH in refluxing EtOH to afford either the dianionic species [7-(PhCC)-8-Ph-7,8-*nido*-$C_2B_9H_9]^{2-}$ **1** if >6 equivalents of KOH are used, or the partially protonated product [7-(PhCC)-8-Ph-7,8-*nido*-$C_2B_9H_{10}]^-$ if only 2 equivalents of KOH are employed. The dianion is obtained in only modest yield, but is conveniently isolated as its Tl^+ salt, a pale yellow solid which is a suitable starting point for the synthesis of transition-metal compounds of **1**. The protonated product is afforded in good yield and may be characterised as alkylammonium salts soluble in halogenated organic solvents. The ^{11}B-{^1H} NMR spectrum of the $[NEt_3H]^+$ salt confirms its *nido* character and asymmetry. Although the ^{11}B spectrum reveals that each boron atom carries an *exo* terminal H atom, no additional coupling, or even broadening, of any of the signals is apparent due to the tenth cage H atom.

The reaction of Tl_2[7-(PhCC)-8-Ph-7,8-*nido*-$C_2B_9H_9$] with [{$RuCl_2$(cym)}$_2$] in CH_2Cl_2 followed by work-up involving TLC affords the orange carbametallaborane [1-(PhCC)-2-Ph-3-(cym)-3,1,2-$RuC_2B_9H_9$] **2** in modest yield. Proton NMR spectroscopic data are consistent with one cym ligand to two Ph groups. The ^{11}B-{^1H} NMR spectrum reveals five resonances with relative integrals 1:1:2:4:1 (high to low frequency), the peaks of integral 2 and 4 being unresolved coincidences at 128.4 MHz.

In recent papers[4–7] we have noted that *pseudocloso* carbametallaboranes **II** are characterised by a weighted average ^{11}B NMR chemical shift, ⟨δ(^{11}B)⟩, of the order of *ca.* 15 ppm higher in frequency than those of comparable *closo* carbametallaboranes **I**. Thus, for the previously reported species [3-(cym)-3,1,2-*closo*-$RuC_2B_9H_{11}$][8] and [1-Ph-3-(cym)-3,1,2-*closo*-$RuC_2B_9H_{10}$][8] ⟨δ(^{11}B)⟩ is −9.58 and −8.04 ppm, respectively, whilst for [1,2-Ph_2-3-(cym)-3,1,2-*pseudocloso*-$RuC_2B_9H_9$][5] ⟨δ(^{11}B)⟩ is +5.58 ppm. Replacement of a phenyl substituent on a carbaborane by a phenylethynyl substituent could reasonably be expected to result in an average increased shielding of the boron nuclei by *ca.* 1 ppm, comparing ⟨δ(^{11}B)⟩ for 1,2-Ph_2-1,2-$C_2B_{10}H_{10}$ (−7.64 ppm) with that for 1-PhCC-2-Ph-1,2-$C_2B_{10}H_{10}$ (−8.70 ppm). On this basis, were compound **2** to have a full *pseudocloso* structure, ⟨δ(^{11}B)⟩ would be anticipated to be *ca.* +4 to +5 ppm. That observed is only +2.41 ppm, a value clearly too high for a *closo* carbametallaborane and rather low for a *pseudocloso* one, but reasonable if an intermediate structure was adopted.

Confirmation of such an intermediate, *semipseudocloso*, structure for compound **2** was derived from crystallographic

Table 1 Crystallographic data and details of data collection and structure refinement for compound **2**

Formula	$C_{26}H_{33}B_9Ru$
M	543.88
Crystal size/mm	0.20 × 0.25 × 0.40
System	Orthorhombic
Space group	*Pbca*
a/Å	12.8309(12)
b/Å	18.1447(11)
c/Å	22.961(2)
U/Å^3	5345.5(8)
Z	8
D_c/g cm^{-3}	1.352
μ(Mo-Kα)/mm^{-1}	0.601
F(000)	2224
$\theta_{orientation}$/°	8–11
$\theta_{data\ collection}$/°	1.77–25.01
hkl Ranges	−1 to +21, −1 to +15, −1 to +27
Data measured	5784
Unique data	4707
Data observed [$I \geqslant 2\sigma(I)$]	2690
g_1	0.467
g_2	0.0
R (all data)	0.0916
R (observed data)	0.0411
$wR(F^2)$	0.1077
S	1.046
Variables	325
Maximum, minimum residues/ e Å^{-3}	0.255, −0.313

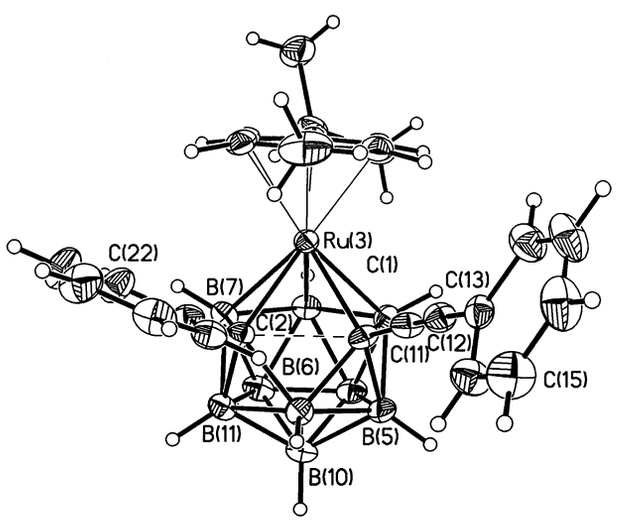

Fig. 1 Perspective view of a single molecule of compound **2** (30% thermal ellipsoids except for hydrogen atoms which have an artificial radius of 0.1 Å for clarity). The phenyl rings are numbered cyclically [C(13)–C(18), C(21)–C(26) and C(31)–C(36)]. Cage and phenyl hydrogen atoms carry the same number as the atom to which they are attached

study. Fig. 1 views a single molecule and demonstrates the atomic numbering scheme adopted, whilst Table 2 presents selected molecular parameters. It is immediately apparent that the C(1)–C(2) connectivity in **2**, 2.184(7) Å, is substantially extended relative to that in 1-PhCC-2-Ph-1,2-$C_2B_{10}H_{10}$,[14] 1.710(2) Å, and to that in the related *closo* carbaruthenaboranes [3-C_6H_6-3,1,2-$RuC_2B_9H_{11}$],[15] 1.626(4) Å, [3-C_6Me_6-3,1,2-$RuC_2B_9H_{11}$],[16] 1.657(10) Å, [1-Ph-3-(mes)-3,1,2-$RuC_2B_9H_{10}$] (mes = mesitylene, $C_6H_3Me_3$-1,3,5),[8] 1.656(6) Å and even [1-Ph-2-Me-3-(cym)-3,1,2-$RuC_2B_9H_9$],[8] 1.702(10) and 1.754(11) Å where a sterically driven incipient C(1)–C(2) lengthening has been noted. At the same time, C(1)–C(2) in **2** is significantly less than that in the full *pseudocloso* carbaruthenaboranes [1,2-Ph_2-3-(cym)-3,1,2-$RuC_2B_9H_9$] and [1,2-Ph_2-3-C_6H_6-3,1,2-$RuC_2B_9H_9$], 2.453(5) and 2.485(8) Å respectively.[5]

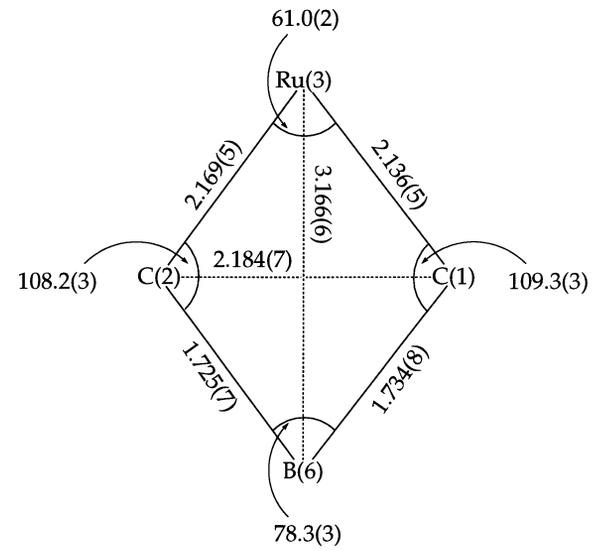

Fig. 2 Geometrical details (Å and °) in the open face of the *semipseudocloso* compound **2**

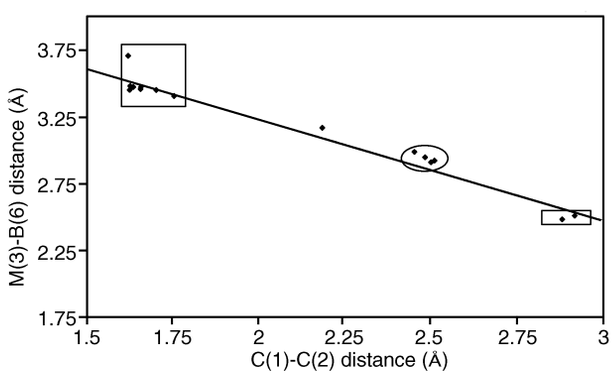

Fig. 3 Plot of C(1)–C(2) distance *versus* M(3)–B(6) distance in compound **2** and typical *closo* (enclosed within square), *pseudocloso* (ellipse) and *hypercloso* (rectangle) 12-vertex carbametallaboranes: *closo* species, [3-(C_6H_6)-3,1,2-$RuC_2B_9H_{11}$],[15] [3-(C_6Me_6)-3,1,2-$RuC_2B_9H_{11}$],[16] [1-Ph-3-(mes)-3,1,2-$RuC_2B_9H_{10}$],[8] [1-Ph-2-Me-3-(cym)-3,1,2-$RuC_2B_9H_9$],[8] [3-(C_5Me_5)-3,1,2-$RhC_2B_9H_{11}$],[17] [3-(C_5Me_5)-3,1,2-$IrC_2B_9H_{11}$][17] and [1,2-Me_2-3-{$(Me_3P)(CO)_2(\mu$-H)$Pt(PEt_3)_2$}-3,1,2-$WC_2B_9H_8$-($CH_2C_6H_4Me$)];[18] *pseudocloso* species, [1,2-Ph_2-3-(C_6H_6)-3,1,2-$RuC_2B_9H_9$],[5] [1,2-Ph_2-3-(cym)-3,1,2-$RuC_2B_9H_9$][5] and [1,2-Ph_2-3-(C_5Me_5)-3,1,2-$RhC_2B_9H_9$];[4] *hypercloso* species, [{$(\mu$-CO)$_2$Pt(PEt_3)$_2$}-$WC_2B_9H_8(CH_2C_6H_4Me)Me_2$][18] and [$W_2(\mu$-$CC_6H_4Me)(\mu$-CO)$_2$($C_2B_9H_9$-$Me_2$){$C_2B_9H_8(CH_2C_6H_4Me)Me_2$}]$^-$[19]

In *pseudocloso* compounds a nearly square M(3)C(1)B(6)-C(2) face is generated, and the M(3)···B(6) distance is reduced from typically 3.5 Å in *closo* 12-vertex carbametallaboranes to <3 Å. In **2** Ru(3)···B(6) is 3.166(6) Å. Overall the M(3)C(1)B(6)C(2) unit, which is sketched in Fig. 2, appears geometrically to have been distorted towards square whilst retaining definite diamond character. *pseudocloso* Carbametallaboranes prepared so far all have 1,2-Ph_2-3-L-3,1,2-MC_2B_9 skeletons, in which the steric demand of the metal-bonded ligand L has forced the cage phenyl substituents to adopt high θ_{Ph} values and so push against each other, breaking the C(1)–C(2) connectivity. In **2** θ_{Ph} is similarly high, 66.8(7)°, but now the cage-bound Ph group pushes against the π-electron density in the C(11)≡C(12) ethynyl group. This presumably results in rather less steric crowding than between two high θ_{Ph} phenyl groups and limits the structural deformation from *closo* to *semipseudocloso*.

Fig. 3 plots C(1)–C(2) distance *versus* M(3)–B(6) distance for compound **2** and typical 12-vertex *closo*, *pseudocloso* and *hypercloso* carbametallaboranes. Data for the last three are

Table 2 Selected interatomic distances (Å) and interbond angles (°) for compound **2**

C(1)–C(11)	1.436(7)	C(1)–B(5)	1.644(7)	B(4)–B(12)	1.806(8)	B(4)–B(8)	1.811(9)
C(1)–B(4)	1.681(7)	C(1)–B(6)	1.734(8)	B(4)–B(5)	1.816(8)	B(5)–B(10)	1.762(9)
C(1)–Ru(3)	2.136(5)	C(1)–C(2)	2.184(7)	B(5)–B(12)	1.769(9)	B(5)–B(6)	1.799(9)
C(2)–C(21)	1.500(7)	C(2)–B(11)	1.646(7)	B(6)–B(11)	1.780(8)	B(6)–B(10)	1.821(8)
C(2)–B(7)	1.667(7)	C(2)–B(6)	1.725(7)	B(8)–B(9)	1.785(8)	B(8)–B(7)	1.797(8)
C(2)–Ru(3)	2.169(5)	Ru(3)–B(4)	2.194(5)	B(8)–B(12)	1.807(9)	B(9)–B(12)	1.755(9)
Ru(3)–B(7)	2.208(5)	Ru(3)–B(8)	2.214(6)	B(9)–B(10)	1.759(9)	B(9)–B(11)	1.765(8)
Ru(3)–C(33)	2.238(5)	Ru(3)–C(35)	2.243(5)	B(9)–B(7)	1.800(8)	B(10)–B(11)	1.746(9)
Ru(3)–C(36)	2.263(5)	Ru(3)–C(34)	2.270(5)	B(10)–B(12)	1.764(9)	B(11)–B(7)	1.810(8)
Ru(3)–C(32)	2.277(5)	Ru(3)–C(31)	2.322(5)	C(11)–C(12)	1.179(7)	C(12)–C(13)	1.441(7)
C(11)–C(1)–B(5)	118.0(4)	C(11)–C(1)–B(4)	129.0(5)	C(2)–B(6)–B(11)	56.0(3)	C(1)–B(6)–B(5)	55.4(3)
B(5)–C(1)–B(4)	66.2(3)	C(11)–C(1)–B(6)	112.3(4)	B(11)–B(6)–B(10)	58.0(3)	B(5)–B(6)–B(10)	58.2(3)
B(5)–C(1)–B(6)	64.3(3)	C(11)–C(1)–Ru(3)	114.4(3)	B(9)–B(8)–B(7)	60.3(3)	B(9)–B(8)–B(12)	58.5(4)
B(4)–C(1)–Ru(3)	69.0(3)	B(6)–C(1)–Ru(3)	109.3(3)	B(12)–B(8)–B(4)	59.9(3)	B(7)–B(8)–Ru(3)	65.8(3)
C(11)–C(1)–C(2)	121.5(4)	B(6)–C(1)–C(2)	50.6(3)	B(4)–B(8)–Ru(3)	65.2(2)	B(12)–B(9)–B(10)	60.2(4)
Ru(3)–C(1)–C(2)	60.3(2)	C(21)–C(2)–B(11)	119.1(4)	B(10)–B(9)–B(11)	59.4(3)	B(12)–B(9)–B(8)	61.4(4)
C(21)–C(2)–B(7)	126.7(4)	B(11)–C(2)–B(7)	66.2(3)	B(11)–B(9)–B(7)	61.0(3)	B(8)–B(9)–B(7)	60.2(3)
C(21)–C(2)–B(6)	115.5(4)	B(11)–C(2)–B(6)	63.7(3)	B(11)–B(10)–B(9)	60.5(4)	B(9)–B(10)–B(12)	59.8(4)
C(21)–C(2)–Ru(3)	113.7(3)	B(7)–C(2)–Ru(3)	68.8(3)	B(5)–B(10)–B(12)	60.2(3)	B(11)–B(10)–B(6)	59.8(3)
B(6)–C(2)–Ru(3)	108.2(3)	C(21)–C(2)–C(1)	123.9(4)	B(5)–B(10)–B(6)	60.3(3)	B(10)–B(11)–B(9)	60.1(4)
B(6)–C(2)–C(1)	51.0(3)	Ru(3)–C(2)–C(1)	58.8(2)	C(2)–B(11)–B(6)	60.3(3)	B(10)–B(11)–B(6)	62.2(3)
C(1)–Ru(3)–C(2)	61.0(2)	C(1)–Ru(3)–B(4)	45.6(2)	C(2)–B(11)–B(7)	57.5(3)	B(9)–B(11)–B(7)	60.4(3)
C(2)–Ru(3)–B(7)	44.8(2)	B(4)–Ru(3)–B(8)	48.5(2)	B(8)–B(7)–B(9)	59.5(3)	C(2)–B(7)–B(11)	56.3(3)
B(7)–Ru(3)–B(8)	48.0(2)	C(35)–Ru(3)–C(36)	35.8(2)	B(9)–B(7)–B(11)	58.6(3)	C(2)–B(7)–Ru(3)	66.4(2)
C(33)–Ru(3)–C(34)	36.5(2)	C(35)–Ru(3)–C(34)	36.4(2)	B(8)–B(7)–Ru(3)	66.2(3)	B(9)–B(12)–B(10)	60.0(4)
C(33)–Ru(3)–C(32)	35.8(2)	C(36)–Ru(3)–C(31)	36.0(2)	B(10)–B(12)–B(5)	59.8(4)	B(5)–B(12)–B(4)	61.1(3)
C(32)–Ru(3)–C(31)	35.7(2)	B(12)–B(4)–B(8)	60.0(3)	B(9)–B(12)–B(8)	60.1(3)	B(4)–B(12)–B(8)	60.2(3)
C(1)–B(4)–B(5)	55.9(3)	B(12)–B(4)–B(5)	58.5(3)	C(12)–C(11)–C(1)	174.1(6)	C(11)–C(12)–C(13)	176.3(6)
C(1)–B(4)–Ru(3)	65.3(2)	B(8)–B(4)–Ru(3)	66.3(3)	C(14)–C(13)–C(17)	117.8(5)	C(14)–C(13)–C(12)	119.7(5)
B(10)–B(5)–B(12)	59.9(3)	C(1)–B(5)–B(6)	60.3(3)	C(17)–C(13)–C(12)	122.4(6)	C(22)–C(21)–C(26)	118.6(5)
B(10)–B(5)–B(6)	61.5(3)	C(1)–B(5)–B(4)	57.9(3)	C(22)–C(21)–C(2)	119.8(5)	C(26)–C(21)–C(2)	121.6(5)
B(12)–B(5)–B(4)	60.5(3)	C(2)–B(6)–C(1)	78.3(3)				

Table 3 Root-mean-square misfits (Å) between the 12-vertex cores of compound **2** and typical *closo* and *pseudocloso* carbaruthenaboranes *

		Individual atom misfit											
Comparison	r.m.s. misfit	C(1)	C(2)	Ru(3)	B(4)	B(5)	B(6)	B(7)	B(8)	B(9)	B(10)	B(11)	B(12)
2/**3**	0.135	0.277	0.263	0.155	0.084	0.031	0.168	0.069	0.042	0.018	0.053	0.054	0.020
2/**4**	0.073	0.115	0.155	0.092	0.035	0.028	0.111	0.025	0.032	0.028	0.032	0.018	0.025
3/**4**	0.204	0.409	0.428	0.255	0.083	0.090	0.247	0.071	0.096	0.039	0.051	0.074	0.043

* Compound **3** is [1-Ph-3-(mes)-3,1,2-*closo*-$RuC_2B_9H_{10}$][8] and **4** is [1,2-Ph_2-3-(cym)-3,1,2-*pseudocloso*-$RuC_2B_9H_9$].[5] For a description of the r.m.s. misfit method see ref. 20.

clustered together by type and there is a reasonable linear relationship between the two distances over all three families (correlation coefficient = −0.98). Compound **2** clearly falls outside the three clusters but close to the line; it sits between *closo* and *pseudocloso*, but nearer to the latter.

Previously[20] we have demonstrated the utility of the root-mean-square (r.m.s.) misfit method to distinguish between geometrically similar but electronically different borane fragments, and it is instructive to apply such calculations to the present study. In Table 3 are presented the overall r.m.s. misfits and individual atom misfits arising from comparisons of the crystallographically determined {3,1,2-RuC_2B_9} fragments of **2**, [1-Ph-3-(mes)-3,1,2-$RuC_2B_9H_{10}$][8] **3** and [1,2-Ph_2-3-(cym)-3,1,2-$RuC_2B_9H_9$][5] **4**, the last two being used as reference *closo* and *pseudocloso* species respectively. In all comparisons the greatest misfitting atoms are C(1) and C(2), followed by Ru(3) and B(6), showing that these sterically derived distortions are localised to the M(3)C(1)B(6)C(2) diamond/square. Compound **2** fits somewhat better with **4** than with **3**, *i.e.* it is geometrically closer to *pseudocloso* than *closo* (*ca.* 65% *pseudocloso*, 35% *closo*), supporting the conclusion from Fig. 2. The fact that **2** lies on a direct pathway between **3** and **4** is illustrated by the extent to which the **2**/**3** and **2**/**4** r.m.s. misfits sum almost exactly to the **3**/**4** r.m.s. misfit.

Thus the results of the NMR and crystallographic studies on compound **2** are entirely consistent: the molecule is distorted by steric crowding into a *semipseudocloso* shape which appears to lie between *closo* and *pseudocloso*, albeit somewhat closer to the latter. These results provide excellent evidence for a continuum of cluster shapes between these forms, the position on which of an individual molecule could, in principle, be controlled by judicious choice of substituent groups. Future contributions will describe attempts to exploit this control, particularly in the fascinating area of sterically induced polyhedral isomerisations.[21,22]

Acknowledgements

We thank Heriot-Watt University for provision of a studentship (for Rh. Ll. T.), Dr. J. Cowie for useful discussions and the Callery Chemical Company for a generous gift of $B_{10}H_{14}$.

References

1 Part 14, G. M. Rosair, A. J. Welch, A. S. Weller and S. K. Zahn, *J. Organomet. Chem.*, in the press.
2 Z. G. Lewis and A. J. Welch, *Acta Crystallogr., Sect. C*, 1993, **49**, 705.
3 J. Cowie, D. J. Donohoe, N. L. Douek and A. J. Welch, *Acta Crystallogr., Sect. C*, 1993, **49**, 710.
4 Z. G. Lewis and A. J. Welch, *J. Organomet. Chem.*, 1992, **430**, C45.

5 P. T. Brain, M. Bühl, J. Cowie, Z. G. Lewis and A. J. Welch, *J. Chem. Soc., Dalton Trans.*, 1996, 231.
6 U. Grädler, A. S. Weller, A. J. Welch and D. Reed, *J. Chem. Soc., Dalton Trans.*, 1996, 335.
7 A. S. Weller and A. J. Welch, *Inorg. Chem.*, 1996, **35**, 4538.
8 J. Cowie, B. D. Reid, J. M. S. Watmough and A. J. Welch, *J. Organomet. Chem.*, 1994, **481**, 283.
9 D. M. Murphy, D. M. P. Mingos, J. L. Haggitt, H. R. Powell, S. A. Westcott, T. B. Marder, N. J. Taylor and D. R. Kanis, *J. Mater. Chem.*, 1993, **3**, 139.
10 M. A. Bennett, T.-N. Huang, T. W. Matheson and A. K. Smith, *Inorg. Synth.*, 1982, **21**, 74.
11 XSCANS, Siemens Analytical Instruments Inc., Madison, WI, 1994.
12 XPREP, Siemens Analytical Instruments Inc., Madison, WI, 1994.
13 SHELXTL (PC version 5.0), Siemens Analytical Instruments Inc., Madison, WI, 1994.
14 W. Clegg, R. Coult, M. A. Fox, W. R. Gill, J. A. H. MacBride and K. Wade, *Polyhedron*, 1993, **12**, 2711.
15 M. P. Garcia, M. Green, F. G. A. Stone, R. G. Somerville, A. J. Welch, C. E. Briant, D. N. Cox and D. M. P. Mingos, *J. Chem. Soc., Dalton Trans.*, 1985, 2343.
16 X. L. R. Fontaine, N. N. Greenwood, J. D. Kennedy, J. Plesek, B. Stibr and M. Thornton-Pett, *Acta Crystallogr., Sect. C*, 1990, **46**, 995.
17 X. L. R. Fontaine, N. N. Greenwood, J. D. Kennedy, K. Nestor, M. Thornton-Pett, S. Hermanek, T. Jelinek and B. Stibr, *J. Chem. Soc., Dalton Trans.*, 1990, 681.
18 M. J. Attfield, J. A. K. Howard, A. N. de M. Jelfs, C. M. Nunn and F. G. A. Stone, *J. Chem. Soc., Dalton Trans.*, 1987, 2219.
19 N. Carr, D. F. Mullica, E. L. Sappenfield and F. G. A. Stone, *Organometallics*, 1992, **11**, 3697.
20 S. A. Macgregor, A. J. Wynd, N. Moulden, R. O. Gould, P. Taylor, L. J. Yellowlees and A. J. Welch, *J. Chem. Soc., Dalton Trans.*, 1991, 3317.
21 D. R. Baghurst, R. C. B. Copley, H. Fleischer, D. M. P. Mingos, G. O. Kyd, L. J. Yellowlees, A. J. Welch, T. R. Spalding and D. O'Connell, *J. Organomet. Chem.*, 1993, **447**, C14.
22 T. D. McGrath and A. J. Welch, *J. Chem. Soc., Dalton Trans.*, 1995, 1755.

Received 10*th September* 1996; *Paper* 6/06258*J*